

Subtle dimensions of climate change have strong
demographic effects on a cactus population in
extinction debt

Kevin Czachura and Tom E.X. Miller*

Program in Ecology and Evolutionary Biology, Department of
BioSciences, Rice University, Houston, TX USA

*Corresponding author: tom.miller@rice.edu (1-713-348-4218)

Abstract

- 1 1. The effects of climate change on population viability reflect the net influ-
2 ence of potentially diverse responses of individual-level demographic pro-
3 cesses (growth, survival, regeneration) to multiple components of climate.
4 Articulating climate-demography connections can facilitate forecasts of re-
5 sponses to future climate change as well as back-casts that may reveal how
6 populations responded to historical climate change.
- 7 2. We studied climate-demography relationships in the cactus *Cyclindriopun-*
8 *tia imbricata*; previous work indicated that our focal population has high
9 abundance but a negative population growth rate, where deaths exceed
10 births, suggesting that it persists under extinction debt. We parameter-
11 ized a climate-dependent integral projection model with data from a 14-year
12 field study, then back-casted expected population growth rates since 1900
13 to test the hypothesis that recent climate change has driven this population
14 into extinction debt.
- 15 3. We found clear patterns of climate change in our central New Mexico study
16 region but, contrary to our hypothesis, *C. imbricata* has most likely bene-
17 fitted from recent climate change and is on track to reach replacement-level
18 population growth within 38 years, or sooner if climate change accelerates.
19 Furthermore, the strongest feature of climate change (a trend toward years
20 that are overall warmer and drier, captured by the first principal component
21 of inter-annual variation) was not the main driver of population responses.
22 Instead, temporal trends in population growth were dominated by more sub-

23 tle, seasonal climatic factors with relatively weak signals of recent change
24 (wetter and milder cool seasons, captured by the second and third principal
25 components).

26 4. *Synthesis*. Our results highlight the challenges of forecasting population dy-
27 namics under climate change, since the most apparent features of climate
28 change may not be the most important drivers of ecological responses. Envi-
29 ronmentally explicit demographic models can help meet this challenge, but
30 they must consider the magnitudes of different aspects of climate change
31 alongside the magnitudes of demographic responses to those changes.

32 **Keywords**

33 Cactaceae; Climate change; Demography; Extinction debt; Integral Projection
34 Model; Long-term ecological research

Introduction

Population extinction debt is likely to increase in frequency as a fingerprint of global change, including climate change (Dullinger *et al.*, 2012; Urban, 2015). Extinction debt is a form of transient dynamics whereby populations persist despite having population growth rates that fall below replacement level ($\lambda < 1$), suggesting a long-term trajectory toward local extinction but with potentially long time lags (Hastings *et al.*, 2018; Kuussaari *et al.*, 2009). While extinction debt is often studied through species richness patterns at the community level (e.g., Vellend *et al.* 2006), there is recent emphasis on the underlying single-species dynamics whereby populations transition from positive to negative growth rates (Lehtilä *et al.*, 2016; Hylander & Ehrlén, 2013). In the absence of significant migration (which can maintain populations in sink habitats), extinction debt suggests that the environment was more favorable for population growth at some time in the past. However, the mechanisms that cause populations to tip from positive to negative growth rates are rarely known, and this information may be critical for effective conservation planning (Hylander & Ehrlén, 2013).

Structured population models built from individual-level demographic rates provide a powerful framework for studying drivers of extinction debt (Lehtilä *et al.*, 2016) and environment-dependent population dynamics more generally (Ehrlén & Morris, 2015). By incorporating climatic factors as statistical covariates, previous studies have identified climatic limits of population viability and forecasted responses to particular types of climate change (e.g., Adler *et al.* 2013; Maschinski *et al.* 2006; Jenouvrier *et al.* 2014). Additionally, articulating the connections between environment and demography can allow for ‘back-casting’ popu-

59 lation dynamics into historical environmental regimes; while rarely done (Smith
60 *et al.*, 2005), this approach may provide valuable insight regarding when and why
61 populations fell into extinction debt.

62 Many studies of climate-demography relationships focus on single climate vari-
63 ables that are known to be a dominant component of climate change and / or
64 known to have a strong influence on the focal species (e.g., Van de Pol *et al.* 2010;
65 Iler *et al.* 2019; Jenouvrier *et al.* 2009). However, for many species, it is not always
66 apparent *a priori* which dimensions of climate are most important, and this poses
67 challenges for predicting population responses to climate change. Previous studies
68 have shown that different components of climate change may have independent
69 effects on different aspects of demography or physiology (Buckley & Kingsolver,
70 2012; Frederiksen *et al.*, 2008; Van de Pol *et al.*, 2010; Lynch *et al.*, 2014). Fur-
71 thermore, different life stages (e.g., young vs old) and different vital rate processes
72 (e.g., growth, survival, reproduction) may differ in the magnitude and even di-
73 rection of their responses to single climate drivers (Doak & Morris, 2010; Dybala
74 *et al.*, 2013; Morrison & Hik, 2007; Tenhumberg *et al.*, 2018), and single life stages
75 or vital rates may be affected by multiple drivers (Dalglish *et al.*, 2011; Williams
76 *et al.*, 2015; Frederiksen *et al.*, 2008; Sletvold *et al.*, 2013). Ultimately, the influ-
77 ence of climate on population growth depends on the sensitivities of vital rates
78 to climate drivers and the sensitivities of λ to the vital rates, integrated across the
79 life cycle (McLean *et al.*, 2016; Ådahl *et al.*, 2006). These complications, common
80 to environmentally explicit demographic studies (Ehrlén *et al.*, 2016), highlight
81 the value of leveraging long-term data to gain resolution of climate drivers and the
82 importance of accounting for demographic complexity across the life cycle.

83 We used long-term demographic data to study climate-dependent population

84 dynamics of a long-lived Chihuahuan desert cactus persisting under extinction
 85 debt. Our previous work with the tree cholla cactus (*Cylindriopuntia imbricata*
 86 Haw. D.C.) (Cactaceae) indicated, with >95% certainty, that our focal population
 87 in the northern Chihuahuan Desert (New Mexico, USA) is in decline (stochastic
 88 population growth rate $\lambda_S < 1$) despite current densities that are reasonably high
 89 (Ohm & Miller, 2014; Miller *et al.*, 2009; Elderd & Miller, 2016). This region has
 90 experienced strong climatic fluctuations over the past century, including several
 91 decadal-scale droughts interrupted by relatively wet periods (Peters *et al.*, 2015).
 92 Recent and projected climate change in our study region includes increases in
 93 temperature and shifts in the seasonal timing of precipitation (Petrie *et al.*, 2014;
 94 Cook & Seager, 2013; Cook *et al.*, 2015).

95 Our study was conducted in the following steps. First, we characterized cli-
 96 mate variation and change in our northern Chihuahuan desert study region over
 97 the past century. Second, we estimated vital rate responses to inter-annual climate
 98 variation during the demographic study period (2004–2017). Following previous
 99 studies, we hypothesized that high-sensitivity vital rates (those that strongly influ-
 100 ence λ) would be less responsive environmental variability than low-sensitivity vital
 101 rates (Pfister, 1998). Third, we back-casted climate-dependent demography to
 102 determine whether the past century included periods that were favorable for pop-
 103 ulation growth, thus testing the hypothesis that recent climate change has driven
 104 this population into extinction debt. Our analysis relied on a Bayesian framework
 105 that incorporates key sources of uncertainty into our back-cast. Finally, we asked
 106 whether the components of climate that are changing most strongly are the same
 107 climate components that most strongly influence cactus demography.

Materials and methods

Focal species, study site, and demographic data collection

Tree cholla cactus is widely distributed throughout desert and grassland habitats of the southwest U.S. and northern Mexico. These long-lived plants (40-plus years) grow through the production and elongation of cylindrical stem segments. These vegetative structures as well as flowerbuds are initiated in late spring. Flowering occurs in early summer and stem segment elongation takes place during the remainder of the growing season. For climate analyses, we divide the calendar year into warm-season months (May through September), when stem elongation, flowering, and seed production occur, and cool-season months (October through April).

This study was conducted at the Sevilleta National Wildlife Refuge (SNWR), a Long-Term Ecological Research site (SEV-LTER) in central New Mexico and near the center of this species' geographic distribution. Our study population occurs in the Los Piños mountains at an elevation of 1790 m. Tree cholla are a dominant component of the vegetation in this area (0.1 m^{-2} : Miller *et al.* 2009), along with oaks, yucca, Piñon pine, and the grasses *Bouteloua gracilis* and *B. eriopoda*.

The present study relies on long-term (2004–2017) demographic data on individual-level measures of growth, survival, and reproduction recorded from tagged plants in the Los Piños population that were censused in late May each year. This was a pre-breeding census that corresponds to the initiation of vegetative and reproductive structures (Fig. C1). We treat May 1 as the start of the transition year (coincident with the start of the warm-season months). There were a total of 1172 unique individuals in the data set and 7442 transition-year observations from 4–8

plots or spatial blocks depending on the year. Full details of the study design and data collection are given elsewhere (Miller *et al.*, 2009; Ohm & Miller, 2014; Elderd & Miller, 2016).

Climate data

Our goal was to connect inter-annual variation in demography to corresponding variation in temperature and precipitation. SEV-LTER collects climate data from a network of meteorological stations throughout SNWR, with the oldest records coming from the late 1980s. While the SEV-LTER climate data cover years of our demographic data collection, our intention was to back-cast demographic performance farther back into the 20th century. We therefore gathered climate data from ClimateWNA v5.60 (Wang *et al.*, 2016), a software package that uses PRISM (Daly *et al.*, 2008) and WorldClim (Hijmans *et al.*, 2005) data to calculate downscaled data for western North America based on location and elevation, going as far back as 1900. By relying on downscaled, interpolated climate data instead of direct observations from meteorological stations we are trading off local resolution in favor of more historical years of data. We quantified this loss of resolution by comparing predictions from ClimateWNA to SEV-LTER data for years that they over-lapped, using the SEV-LTER meteorological station that was nearest our study population (Appendix A). We found that the two data sets were highly correlated (Table A1, Figure A1), which bolstered our confidence that ClimateWNA provided locally accurate climate data for both the demographic observation period as well as historical years that preceded our study. We derived seasonal estimates (warm- and cool-season) of total precipitation and mean, minimum, and maximum tem-

155 perature from monthly climate data, for a total of eight variables. Months were
156 aligned to correspond to demographic transition years rather than calendar years,
157 which means the cool-season climate for a transition year beginning in May of year
158 t spans October of year t through April of year $t + 1$ (Fig. C1).

159 To reduce the dimensionality of the climate data, we conducted Principal Com-
160 ponents Analysis (PCA) on the eight climate variables for the years 1900-2017,
161 with climate values scaled to unit variance. We estimated the variance in the raw
162 climate data explained by each PC and the variable loadings, which give the cor-
163 relations between original variables and PC values. PCA allowed us to rank the
164 magnitudes of multiple aspects of climate variation and change by examining how
165 warm- and cool-season variables loaded onto the ranked PC axes.

166 Statistical estimation of climate-dependence

167 We fit generalized linear mixed effects models in a hierarchical Bayesian framework
168 to quantify climate dependence in demographic vital rates, as captured by three
169 principal components of climatic variability. The choice of three PCs was based
170 on results of parallel analysis (Fig. A2), a statistical method for determining how
171 many components to retain (Franklin *et al.*, 1995). There were four vital rates
172 measured in the long-term study for which we could estimate climate dependence:
173 survival from year t to year $t+1$, individual growth (change in size from year
174 t to year $t+1$), probability of flowering in year t , and the number of flowerbuds
175 produced year in t , given that a plant flowered. Survival and growth from year $t-1$
176 to t were dependent on size in year $t-1$, and the climate covariate corresponded
177 to the climate year $t-1$ to t . Reproductive status and fertility in year t were

178 dependent on size in year t and on climate from $t - 1$ to t . This timing of size
 179 and climate effects was intended to match processes in the population model (Fig.
 180 C1). We did not quantify climate-dependence in seedling recruitment. While we
 181 searched plots each year and added newly detected plants to the census, we could
 182 not confidently assign a birth year to these new additions (seedlings require several
 183 years of growth before they are consistently detectable in our census) so we do not
 184 know the climatic conditions under which they recruited.

185 All of the models for climate-dependent vital rates used the same linear predic-
 186 tor for the expected value (μ) but applied a different link function ($f(\mu)$) depending
 187 on the distribution of the observations:

$$\begin{aligned}
 f(\mu) = & \beta_0 + \beta_1 x + \\
 & \rho_1^1 PC1 + \rho_2^1 PC1^2 + \rho_3^1 x PC1 + \\
 & \rho_1^2 PC2 + \rho_2^2 PC2^2 + \rho_3^2 x PC2 + \\
 & \rho_1^3 PC3 + \rho_2^3 PC3^2 + \rho_3^3 x PC3 + \\
 & \gamma + \tau
 \end{aligned} \tag{1}$$

188 The linear predictor includes a grand mean intercept (β_0) and size-dependent
 189 slope (β_1). The size variable x is the natural logarithm of plant volume ($\log_e(cm^3)$),
 190 which was standardized to mean zero and unit variance for analysis. Other fixed-
 191 effect coefficients (ρ) correspond to climate variables and climate \times size inter-
 192 actions. We include quadratic terms for climate to account for the possibility of
 193 non-monotonic climate responses. Climate coefficient (ρ) superscripts correspond
 194 to each PC, and subscripts correspond to linear, quadratic, and size-interaction ef-

fects. Finally, the linear predictor includes normally distributed random effects for plot-to-plot variation ($\gamma \sim N(0, \sigma_{plot})$) and year-to-year variation that is unrelated to climate effects captured by PCs 1-3 ($\tau \sim N(0, \sigma_{year})$). The year random-effect can be interpreted as inter-annual variability in demography that cannot be explained by the climate PCs. We used stochastic variable selection in a Bayesian framework to reduce model complexity, dropping coefficients that were effectively zero with $\geq 90\%$ certainty. Complete methods for variable selection are provided in Appendix B.

The growth data were normally distributed; this model applied the identity link and included an additional parameter for residual variance. We explored size-dependence in the residual variance of growth (which determines how individuals are distributed around their expected future size) but found that this led to poorer model fits, so we proceeded to assume a constant value. The survival and flowering data were Bernoulli distributed, and these models applied the logit link function. The fertility data (flowerbud counts) were modeled as Poisson-distributed, including an individual-level random effect to account for overdispersion. All coefficients were given vague priors. We evaluated model fits using posterior predictive checks (Elder & Miller, 2016). All models were fit using JAGS (Plummer *et al.*, 2003) and R2JAGS (Su & Yajima, 2012). Analysis code is available at https://github.com/texmiller/cholla_climate_IPM.

215 Demographic modeling

216 Model description

217 The statistical models described above formed the backbone of the integral projec-
218 tion model (IPM) that we used to estimate population growth in variable climate
219 environments. Following previous studies (Compagnoni *et al.*, 2016; Ohm & Miller,
220 2014; Elderd & Miller, 2016), we modeled the life cycle of *C. imbricata* using con-
221 tinuously size-structured plants, $n(x)$, and two discrete seed banks ($B_{1,t}$ and $B_{2,t}$)
222 corresponding to 1 and 2-year old seeds:

$$B_{1,t+1} = \kappa \delta \int_L^U P(x, \mathbf{c}_{t-1}; \alpha_t^P) F(x, \mathbf{c}_{t-1}; \alpha_t^F) n(x)_t dx \quad (2)$$

$$B_{2,t+1} = (1 - \gamma_1 B_{1,t}) \quad (3)$$

223 Functions P and F give the probability of flowering and the number of flower-
224 buds produced, respectively, for an x -sized plant. The vector \mathbf{c}_{t-1} contains the
225 climate PC values for climate-year $t - 1$, which affects flowering and fertility in
226 year t , and hence the 1-year old seed bank in year $t + 1$. Parameters α_t^P and α_t^F are
227 random year effects estimated from the statistical models. The integral is multi-
228 plied by the number of seeds per fruit (κ) and probability of seed dispersal/survival
229 (δ) to give the number of seeds that enter the 1-year old seed bank. Parameters L
230 and U are the lower and upper bounds, respectively, of the plant size distribution.
231 Plants can recruit out of the 1-year old seed bank with probability γ_1 or transition
232 to the 2-year old seed bank with probability $(1 - \gamma_1)$. Seeds in the 2-year old seed
233 bank are assumed to either germinate (probability γ_2) or die.

234 Continuous-size dynamics were given by:

$$n(y)_{t+1} = (\gamma_1 B_{1,t} + \gamma_2 B_{2,t}) \eta(y) \omega + \int_L^U S(x, \mathbf{c}_t; \alpha_t^S) G(y, x, \mathbf{c}_t; \alpha_t^G) n(x)_t dx \quad (4)$$

235 The first term indicates recruitment from the seed banks to size y , where $\eta(y)$
 236 gives the seedling size distribution, assumed normal with mean μ_s and standard
 237 deviation σ_s . Mortality between germination (late summer) and the yearly demo-
 238 graphic census (May) is accounted for with survival probability ω . In the second
 239 term, functions S and G give the probabilities of surviving to year $t+1$ and grow-
 240 ing to size y , respectively, for an x -sized plant in year t . Climate-dependence and
 241 random year effects are included as in Eq. 2, except the timing of climate effects
 242 is shifted such that growth and survival from t to $t+1$ are affected by climate over
 243 the same interval (Fig. C1). As above, survival and growth functions also take
 244 time-varying random intercepts. Field data used to estimate seed and seed bank
 245 parameters are described elsewhere (Compagnoni *et al.*, 2016; Elderd & Miller,
 246 2016). All parameter estimates are provided in Table C1.

247 Model analysis

248 For analysis, we discretized x into n bins, replacing the continuous kernel with an
 249 n -by- n matrix (because our model also included two additional discrete states, the
 250 final projection matrix had dimensions $n+2$ -by- $n+2$). We used $n = 200$ bins. We
 251 extended integration limits L and U to avoid unintentional “eviction” (Williams
 252 *et al.*, 2012).

253 We estimated the asymptotic population growth rate λ as the dominant eigen-

254 value of the discretized IPM kernel. We compared the observed size distribution
 255 and the predicted distribution at the long-term mean climate ($PC_1 = PC_2 =$
 256 $PC_3 = 0$) and found generally good agreement (Fig. C2). We then evaluated how
 257 λ responded to climate variation by first varying each climate PC independently,
 258 holding the other two fixed at their long-term mean. Second, we back-casted λ
 259 over the entire climatological record that we had available (1900–2017), which gen-
 260 erated a time series of λ_t . We used linear regression to test for temporal trends
 261 in λ over this period. We incorporated two types of uncertainty into back-casted
 262 values of λ : imperfect knowledge of the parameter values (“estimation error”) and
 263 year-to-year fluctuations that were not related to climate (“process error”); the
 264 latter was estimated from the variances of random year effects. For the years of
 265 demographic data collection (2004–2017), we additionally quantified the deviations
 266 between predicted λ based solely on climate and “observed” λ that reflects climate
 267 and non-climate year effects (quotations indicate that these are the asymptotic pre-
 268 dictions given the vital rates observed in that year). We also conducted a similar
 269 analysis of λ_S using a 10-year sliding window (Appendix C), and we explored the
 270 consequences of extrapolating vital rate responses to climate values more extreme
 271 than those observed during the study period (Appendix D).

Finally, we used Life Table Response Experiments (LTREs) to decompose
 which combinations of climate PCs and vital rate responses were most strongly
 responsible for temporal fluctuations in the back-casted time series λ_t . We used
 a fixed-design LTRE (Caswell, 2001) where λ_t was defined as a linear function of

climate predictors:

$$\lambda_t = \bar{\lambda} + \sum_{i=1}^3 \gamma_i PC_{i,t} \quad (5)$$

There is no error term because, in this analysis, climate PCs are assumed to be the sole drivers of fluctuations in λ_t . The coefficient for each climate PC was approximated as:

$$\beta_i \approx \sum_{j=1}^n \frac{\partial \bar{\lambda}}{\partial \theta_j} \frac{\partial \theta_j}{\partial PC_i} \quad (6)$$

272 The LTRE approximation is based on the product of the sensitivity of λ to the vital
273 rates (θ), evaluated at the long-term mean climate ($PC_1 = PC_2 = PC_3 = 0$), and
274 the sensitivity of the vital rates to climate, summed over all vital rates n . Because
275 LTRE components are additive, we summed LTRE estimates over the intercept
276 and slope of each vital rate function so that we could interpret the results in terms
277 of vital rate contributions.

278 Results

279 Climate trends

280 Three principal components cumulatively explained 73.3% of the inter-annual vari-
281 ation in climate (Figure 1A). PC1 was dominated by inter-annual differences in
282 temperature and precipitation, regardless of season, and the three components of
283 temperature (mean, min, max) loaded similarly onto this component (Figure 1B).
284 Over the last century, PC1 trends have fluctuated, with prolonged stretches of

285 warm and dry years (the 1950s and early 2000s) and other periods of cool and
286 wet years (early 1900s and 1970s-80s), though the overall temporal trend for PC1
287 is negative. The decline per-year is nearly five times stronger since 1970 com-
288 pared to the long-term average (Fig. 1C), suggesting an accelerating trajectory
289 of warmer and drier years. PC2 was strongly driven by cool-season climate, espe-
290 cially precipitation, such that greater values corresponded to wetter winters with
291 low temperature maxima and high temperature minima (Figure 1B). Warm-season
292 temperatures also loaded positively onto this axis to a lesser degree (Figure 1B).
293 PC2 has increased since 1900 and the change per-year is nearly four times stronger
294 since 1970 (Figure 1D), indicating an accelerating trend of wetter cool seasons with
295 moderate winter temperatures. Lastly, PC3 was correlated with a combination of
296 warm- and cool-season climate variables. The strongest variable loadings on this
297 component were minimum and mean temperatures in the cool season and warm-
298 season precipitation. Temporal trends for PC3 showed weak declines since 1900,
299 corresponding to milder winters with higher minimum and mean temperatures and
300 wetter warm seasons; this trend has been slightly stronger since 1970 (Figure 1E).

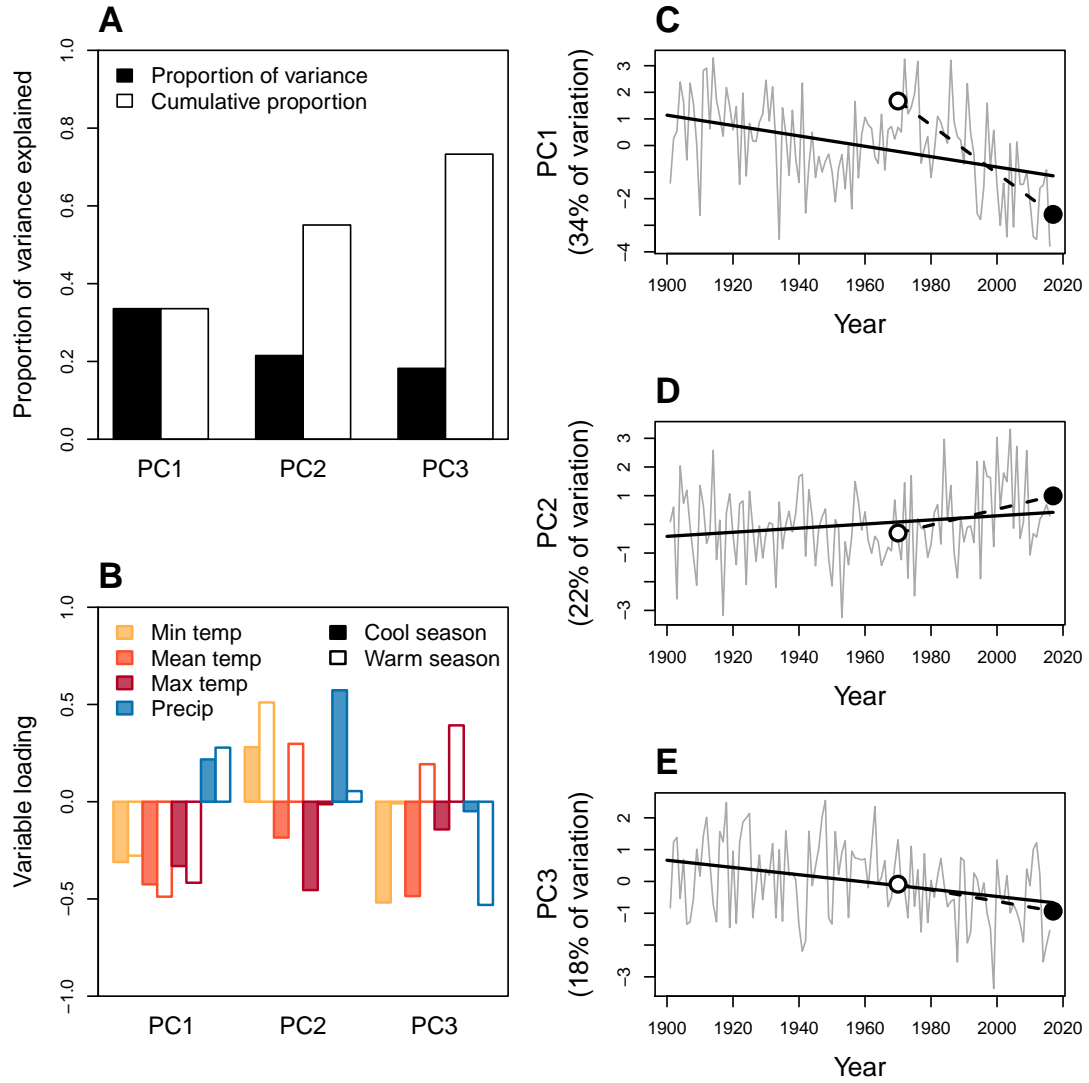


Figure 1: Principal components analysis (PCA) of inter-annual climate variability at SNWR, 1901–2017. **A**, Proportion and cumulative proportion of variation in seasonal temperatures (minimum, mean, maximum) and precipitation explained by the first three PCs. **B**, Loadings of seasonal climate variables onto PC1-3. Because climate data were standardized to mean zero and unit variance, loadings can be interpreted as the correlation between the climate variable and the PC. **C–E**, Time series of PC values, with regression lines showing long-term trends since 1901 (solid lines) or 1970 (dashed lines); open and filled points indicate the years 1970 and 2017, respectively, and correspond to the same shapes in Fig. 3

Vital rate responses to climate

Demographic vital rates estimated from long-term data (survival, growth, reproductive status, and fertility of flowering plants) were least responsive to PC1, the dominant axis of climate variability and change. All of the vital rates were strongly, positively size-dependent but there was heterogeneity in the magnitude and sign of responses to different dimensions of climate variability. Figure 2 shows vital rate data and fitted statistical models following variable selection procedures that eliminated coefficients that were weakly supported (Table B1). There was very little support for coefficients of quadratic climate effects (Table B1), indicating that responses to climate were monotonic over the range of variation we observed.

For PC1, there was a weak reduction in survival probability (especially for smaller plants; Fig. 2A) and a moderate reduction in flowering probability (especially for larger plants; Fig. 2G) at higher PC values, i.e., in cooler and wetter years. Fertility of flowering plants was not responsive to PC1 variation (Fig. 2J) and growth was not responsive to any of the climate PCs (Fig. 2D,E,F). There were positive responses to PC2 in survival (Fig. 2B), flowering probability (Fig. 2H), and fertility of flowering plants (Fig. 2K), indicating that these vital rates benefitted from years with wetter cool seasons. Responses to PC3 varied in sign, with survival increasing with decreasing PC values (years with mild winter temperature minima and wet summers) and reproductive rates increasing with increasing PC values (years with low winter minima and dry summers) (Fig. 2C,I,L).

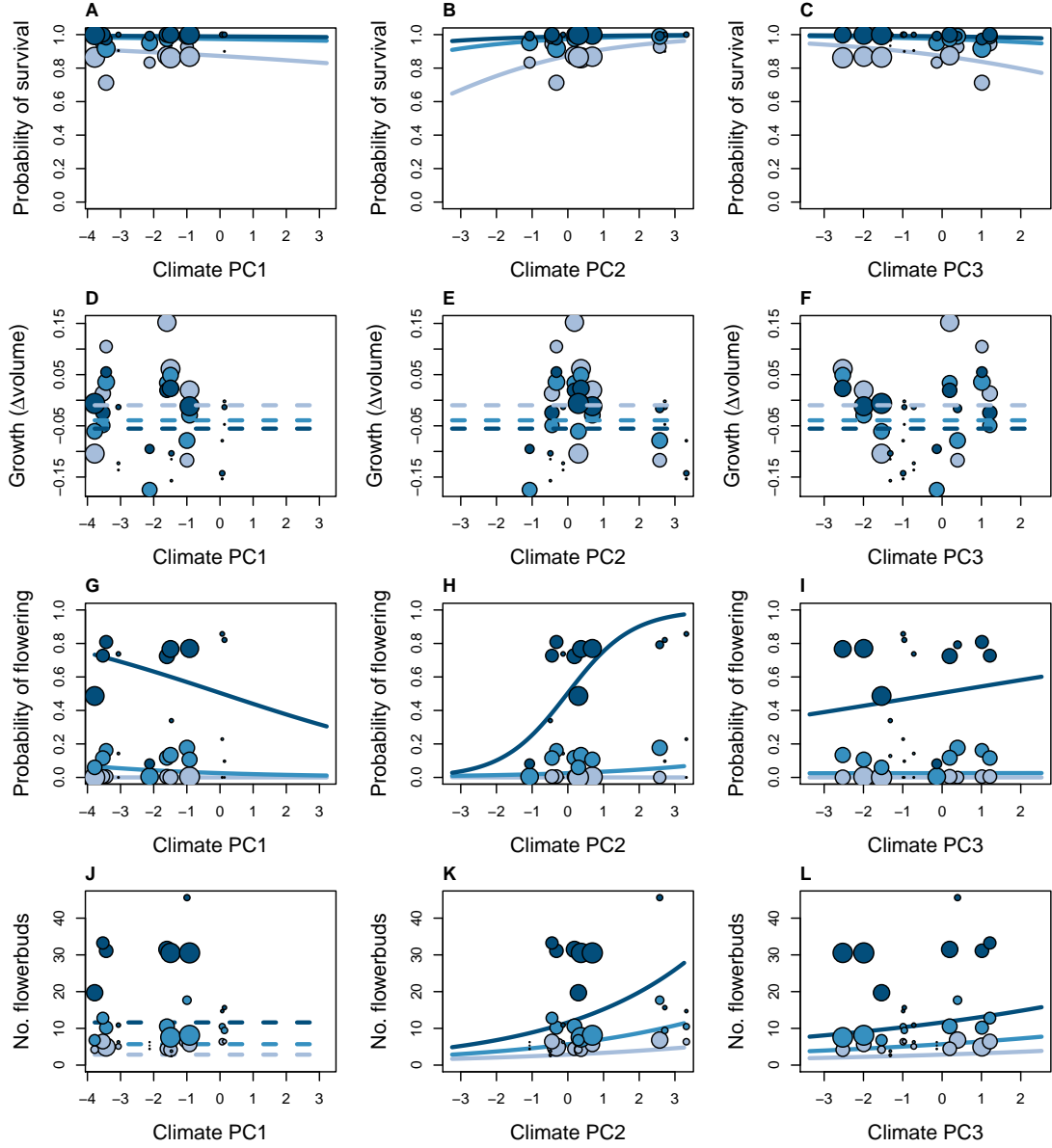


Figure 2: Climate- and size-dependent variation in survival (A-C), growth (D-F), flowering (G-I), and fertility of flowering plants (J-L) in relation to three principal components of seasonal climate variation (columns). For visualization only, the plant size distribution was discretized into three groups (small, medium, and large, corresponding to increasingly dark shading). Points show means for each size group in each year, where different years have unique PC values and point size is proportional to sample size for each size group in each year. Lines show fitted statistical models using posterior mean parameter values, with shading corresponding to size groups. Dashed lines indicate that the climate predictor was not statistically supported. Ranges of x -axes show the climate extrapolation that was required for back-casting.

Climate-dependent population growth

The population growth rate λ was predicted to increase with decreasing values of PC1 (hotter, drier years), holding other PCs fixed at their long-term average (Fig. 3A). Population growth was also predicted to increase with increasing values of PC2 (wetter cool seasons; Fig. 3B). Population growth was more sensitive to PC2 than PC1, such that the predicted change in λ from 1970 to 2017 was slightly greater for PC2 even though PC1 exhibited much greater change than PC2 over this period. Finally, greater values of PC3 (colder winters and drier summers) were predicted to cause declines in population growth, indicating that negative effects on cactus survival outweighed positive effects of PC3 on reproduction (Fig. 2). PC3 has changed relatively little since 1970 but this was associated with a change in λ of about half the magnitude to the response to relatively large change in PC1. Overall, recent climate change in each of the principal components, in isolation, has been in the direction that favors increased population growth (Fig. 1, 3). However, mean estimates for population growth rates were consistently below replacement level for all climate PC values, and the posterior probability densities rarely met or exceeded $\lambda = 1$.

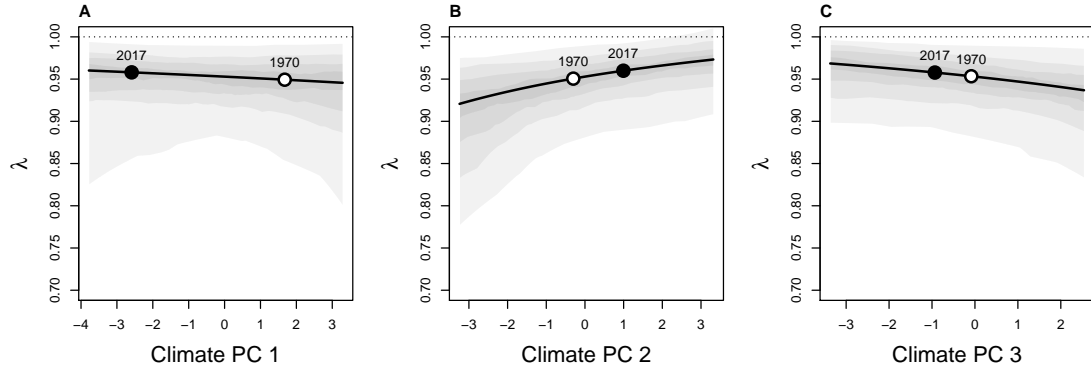


Figure 3: Predicted asymptotic population growth rate (λ) in response to three principal components of inter-annual climatic variation (A-C). For each panel, the indicated principal component is varying while the others are held at zero (the average value). Lines show the expected relationships based on posterior mean parameter values and shaded contours show the 25,50,75, and 95% credible intervals, representing uncertainty in demographic parameters. Points highlight the change the PC value (on the x -axis) between 1970 and 2017, based on the regression lines shown in Fig. 1, and the predicted corresponding change in λ (y -axis).

Back-casting population growth

Figure 4A shows the back-casted time series of λ accounting for inter-annual variation in all three PC components. For the observation years (2004-2017), the three climate PCs explained 57% of the inter-annual variation in λ (points in Fig. 4A). Thus, even with relatively strong climate-demography associations (Fig. 2), there was substantial uncertainty in our back-casted estimates of λ . The shaded region in Fig. 4A represents the combined uncertainty arising from heterogeneity in vital rates across years that could not be attributed to the climate PCs (process error) and imperfect knowledge of the underlying parameters (estimation error). In Appendix Fig. C3, we show that process error contributed the majority of the

349 total uncertainty.

350 Despite uncertainty in our back-cast, the results indicated that λ has likely
351 remained below replacement levels for more than a century; there was no evidence
352 that climate change drove this population into extinction debt. To the contrary,
353 there was a positive temporal trend ($\frac{\Delta\lambda}{\Delta Year} > 0$), suggesting a trajectory of increas-
354 ing population growth rates through time (Fig. 4B). There was wide uncertainty
355 in the rate of change but the posterior probability distribution indicated that it
356 was 2.27 times more likely that λ has increased than decreased. Furthermore, the
357 median rate of increase was 2.76 times greater since 1970 compared to the overall
358 trend since 1900 (Fig. 4B), corresponding to the acceleration of climate change
359 (Fig. 1). There was greater uncertainty in $\frac{\Delta\lambda}{\Delta Year}$ since 1970 because this estimate
360 was based on fewer years. Under the trajectory since 1970, population growth
361 was expected to reach the threshold of positive population growth ($\lambda = 1$) in the
362 year 2057 (Fig. 4C); accelerating climate change would advance this transition to
363 viable growth rates. In Appendix D, we show that our inference that λ is likely
364 increasing in response to climate change holds even with a more conservative ap-
365 proach that does not extrapolate vital rate responses beyond the climate extremes
366 of the observation years.

367 The stochastic population growth rate (λ_S) showed a similar trend of $\lambda_S < 1$
368 and increasing population growth rates over the past 120 years (Fig. C4). The
369 stochastic growth rate reveals the effects of multi-year climate events, such as the
370 runs of good years in the 1940s and 2000s.

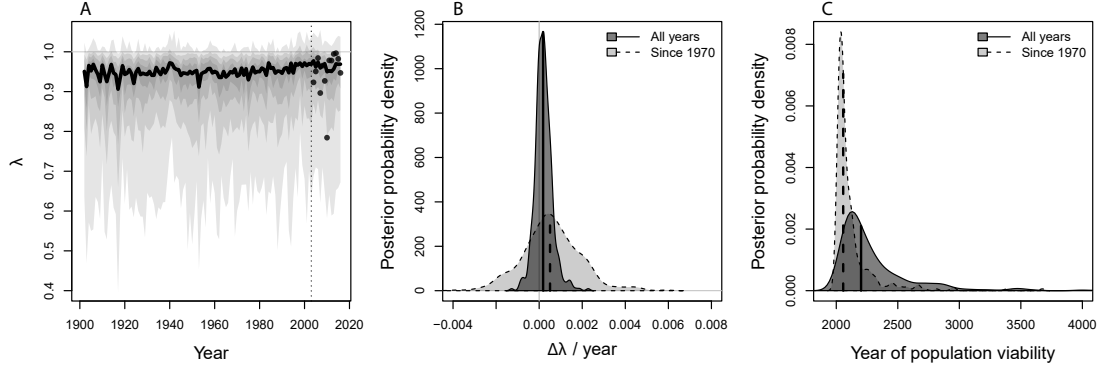


Figure 4: **A**, Posterior probability distribution for the time series of asymptotic population growth rates (λ) predicted based on inter-annual variation in three climate PCs. Thick black line shows the mean prediction and shaded regions show the 25, 50, 75, and 95% credible regions accounting for both parameter uncertainty and process error (year-to-year variation in vital rates that was unrelated to climate). Dashed vertical line separates years that were back-casted versus years that were directly observed. The observation years (2004 and later) include estimates for year-specific population growth rates (points), captured statistically as year-specific random effects in the vital rates. **B**, Posterior distributions for the rate of temporal change in population growth ($\frac{\Delta\lambda}{\Delta Y_{\text{year}}}$). Dark grey shows the rate of change across all years shown in **A** and light grey shows the rate of change since 1970. Vertical lines show median values. **C**, Posterior distributions for the year of population viability ($\lambda = 1$) for the subset of posterior samples for which $\frac{\Delta\lambda}{\Delta Y_{\text{year}}} > 0$. Shading and lines as in **B**.

Life Table Response Experiment

Life Table Response Experiments (LTRE) provided a decomposition of how λ responded to long-term climate trends (1900-2017), allowing us to understand the relative importance of different dimensions of climate variability and vital rate responses to them. LTRE results indicated that survival responses to climate were the overwhelming driver of temporal trends in λ (Fig. 5). Individual growth made no contribution to these trends because it was unresponsive to climate (Fig. D,E,F), whereas flowering and fertility were responsive to climate but their role

379 was relatively small and imperceptible in Fig. 5. Furthermore, survival responses
 380 to climate PC2 were the dominant driver of temporal trends, followed by PC3
 381 and then PC1. Collectively, responses to PC2 and PC3 accounted for 91% of the
 382 overall climate effect in back-casted values of λ .

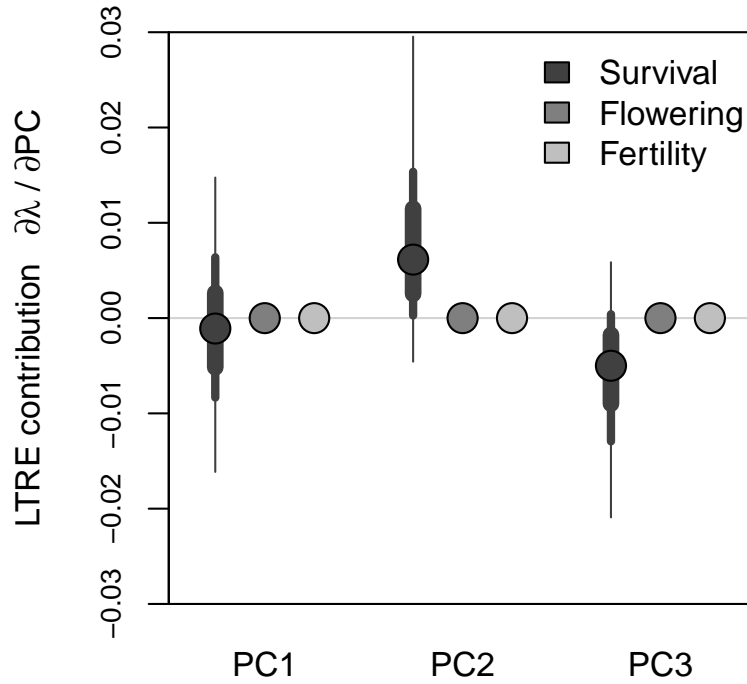


Figure 5: LTR decomposition of climate-driven inter-annual variability in population growth rates. Lines of decreasing thickness show the 50, 75 and 95 percentiles of the posterior distributions of the vital rate parameters, and points show the median. Shading corresponds to different vital rates (survival, flowering, and fertility) Posterior distributions for flowering and fertility are imperceptible on this scale.

Discussion

Understanding and predicting the effects of environmental change on plant demography and population dynamics are urgent challenges. The integration of long-term data with environmentally explicit demographic models provides a powerful vehicle for meeting these challenges and may aid in identifying processes that drive some populations into decline. By reconstructing 117 years of climate-dependent demography, we tested the hypothesis that the extinction debt of our study population was a consequence of recent climate change. Our results suggest the opposite: *C. imbricata* is likely a climate change “winner”, on an accelerating trajectory toward replacement-level within 38 years if current climate change trends persist, and sooner if they accelerate. We further show that the strongest feature of climate change in this system was not the main driver of population responses. Instead, temporal trends in population viability were dominated by more subtle climatic factors with relatively weak signals of recent change. Below, we interpret these results in greater detail and discuss their broader significance.

Until recently, few plant demographic studies explicitly considered climatic drivers of inter-annual variation (Ehrlén *et al.*, 2016; Crone *et al.*, 2011), though this is rapidly changing. We are aware of no previous studies that have compared the magnitudes of different aspects of climate change alongside the magnitudes of demographic responses to those changes. However, we suspect that our key finding – that the strongest dimension of climate change was not the strongest driver of demography – may be common, since at the heart of this result lies the difference between annual climate trends (captured by PC1) versus seasonal trends (PCs 2 and 3). Annual rainfall totals in our region have been decreasing but more of the

annual rainfall has been falling in the cool season, consistent with previous climatological studies that suggest a shift from warm- to cool-season precipitation (Cook & Seager, 2013; Cook *et al.*, 2015; Petrie *et al.*, 2014). Similarly, annual temperatures have been increasing in our study region but it was cool-season warming, specifically, that was most important for *C. imbricata* demography. Many plant and animal life histories operate on seasonal schedules and may therefore be more sensitive to seasonal redistribution of rainfall and temperature than to climate effects that manifest over an entire year. Our results are consistent with previous studies that demonstrate the importance of considering seasonal, not annual, drivers of plant demographic responses (Selwood *et al.*, 2015; Williams *et al.*, 2015; Dahlgren *et al.*, 2016). Some recent studies have taken a finer-grained approach, connecting plant responses to weather events on monthly, weekly, or even daily time scales (Teller *et al.*, 2016; Tenhumberg *et al.*, 2018; Shriver, 2016). For tractability, we did not explore lagged climate effects beyond one year, though methods for doing so are rapidly developing (Teller *et al.*, 2016; Tenhumberg *et al.*, 2018; Ogle *et al.*, 2015). Finding the appropriate timing and resolution of climate covariates is an important area for future work in this system and more generally.

Rigorously accounting for various types of uncertainty is another an important area in the development of environmentally explicit models for forecasting or back-casting. Even with strong climate-demography relationships detected with our unusually long-term data set, climate drivers accounted for little over half of the inter-annual variation in λ during the study years. It was therefore important to place our predictions for historical growth rates in the context of the substantial uncertainty that arose from process error: all the additional, unspecified ways that years may differ. We have emphasized the positive trajectory of population

432 viability as the most likely trend in λ , but this should be interpreted in light
433 of the probability distributions that we provide (Fig. 4) – that is, with nuance
434 and appropriate caution¹. As ecologists are increasingly called upon to forecast
435 responses to change in climate drivers, it will be essential to do so in a probabilistic
436 framework that accommodates process error, i.e., the variability *not* explained by
437 climate drivers.

438 Different aspects of a species' life cycle may respond in diverse ways to environ-
439 mental drivers (Doak & Morris, 2010; Villellas *et al.*, 2015), highlighting the addi-
440 tional importance of considering multiple vital rates for understanding responses
441 to global change. Our work was able to pinpoint which responses throughout the
442 life cycle were most important for the overall population response to climate. Our
443 results are consistent with previous findings that high-sensitivity vital rates (those
444 that strongly influence λ , in this case survival and growth) are buffered against en-
445 vironmental variability while low-sensitivity vital rates (flowering and fertility) may
446 exhibit wide fluctuations (Pfister, 1998). However, incomplete buffering of survival
447 led to greater mortality in years with cold and dry cool-seasons – years that are be-
448 coming less frequent under climate change (Fig. 1) – and these survival responses
449 dominated the overall increase in population viability over the past 120 years
450 (Fig. 5). These results mirror a recent study of another long-lived perennial plant,
451 the alpine sunflower *Helianthella quinquinervis*, where reproductive responses to
452 climate drivers were strong but ultimately overwhelmed by weaker responses in
453 survival that more strongly affected population growth (Iler *et al.*, 2019). It is
454 commonly observed that demographic transitions related to growth and survival

¹The odds that λ is increasing were slightly lower than the odds of a Clinton victory in the 2016 U.S. presidential election: <https://projects.fivethirtyeight.com/2016-election-forecast/>

are the most important determinants of population viability in species with long-lived perennial life histories (Franco & Silvertown, 2004). It may therefore be a general result that climate effects on growth and survival will be more consequential in long-lived perennials than effects on reproductive processes, even as the latter exhibit greater sensitivity to climate, since perennials have many reproductive opportunities over potentially long lifespans (Dalglish *et al.*, 2010; Morris *et al.*, 2008).

Our historical reconstruction of climate-dependent population growth indicated that the climate has likely never been better for *C. imbricata* than it is now. This result begs the question of how these plants have reached their current, relatively high abundance, given over a century of population growth rates that were inferred to fall well below replacement levels. Land use history – which is not incorporated into our back-casted estimates – may have played a role. The Sevilleta NWR was exposed to grazing for much of the 20th century until 1973. Previous work suggests that cacti, and *C. imbricata* in particular, can increase in abundance in response to grazing, due to livestock dispersing detached stem segment and thus promoting asexual regeneration (Allen *et al.*, 1991). During our study, we observed recruitment to be almost exclusively from seed (sexual and asexual recruits are easily distinguishable), though it is possible that regeneration dynamics were different under historical grazing regimes. Grazing may have also promoted cactus populations through release of competitive interactions with grasses (Yu *et al.*, 2019). Thus, one hypothesis is that *C. imbricata* achieved current densities under the historical land use regime, and cannot maintain these densities in the absence of cattle grazing. For long-lived plants, it may take decades to centuries for full payment of extinction debt driven by land use changes (Lehtilä *et al.*,

2016; González-Varo *et al.*, 2015). An alternative hypothesis is that, independent of grazing or other land use history, our study population may be located in sink habitat and maintained by dispersal from nearby populations that are more viable. Indeed, previous work showed that *C. imbricata* at lower elevations had positive population growth rates (Miller *et al.*, 2009) and may therefore act as source populations. Regardless of which process or processes best account for the persistence of a population that is currently inviable, our results indicate that it will likely be ‘rescued’ by ongoing climate change. One caveat to this conclusion is that, beyond the mean climate trends we have described, future climate (and especially monsoon precipitation) in our region is expected to be more variable (Rudgers *et al.*, 2018; Cook *et al.*, 2015) and this may dampen population growth independently of mean conditions (Boyce *et al.*, 2006). However, our stochastic demographic analysis, which accounts for increasing climate variability during the 20th century, also showed a positive trajectory of λ_S (Fig. C4).

Previous studies of cacti have emphasized their sensitivity to freezing as a constraint on physiological performance and geographic distribution (Flores & Yeaton, 2003; Kinraide, 1978; Nobel, 1984). In our study, we detected an important role for winter minimum temperature and observed high mortality following record low winter temperatures over a multi-day deep-freeze in 2011 (this is the low outlier in Fig. 4A). As these freezing events become less frequent under climate change, we expect an increase in regional abundance and perhaps northern expansion of *C. imbricata*’s range, which currently extends to southern Colorado and is likely limited by winter minimum temperatures. This may be an issue of applied concern in the region since *C. imbricata* is considered undesirable, particularly on rangelands (Allen *et al.*, 1991). The role of cool-season precipitation that we detected was

505 more surprising. A majority of annual precipitation in the Southwest US comes
506 from warm-season monsoon events (Adams & Comrie, 1997) and these events
507 play a critical role in vegetation dynamics (Notaro & Gutzler, 2012; Petrie *et al.*,
508 2014), especially for plants with C4 and CAM photosynthesis that are physiologi-
509 cally most active during the warm summer months. Previous cactus demographic
510 studies have emphasized the role of summer monsoon precipitation (Winkler *et al.*,
511 2018; Bowers, 2005). Our results suggest that, despite its summer-adapted CAM
512 photosynthetic pathway, *C. imbricata* is able to capitalize on cool-season mois-
513 ture, and this was an important component of the positive demographic effects
514 of recent climate change. Similarly, Salguero-Gomez *et al.* (2012) identified the
515 desert species *Cryptantha flava* as a climate change winner due in part to seasonal
516 redistribution of rainfall that will lengthen its growing season.

517 Several limitations of our study warrant consideration in the interpretation of
518 our results. First, our consideration of climate dependence was limited to four
519 vital rate processes of established plants. Because we could not reliably assign a
520 birth year to new recruits, we did not incorporate climate dependence in seedling
521 recruitment. Previous studies of cactus demography suggest that seedling recruit-
522 ment may be highly sensitive to climate, especially monsoon precipitation (e.g.,
523 Bowers 2005; Winkler *et al.* 2018). We suspect this is the case for *C. imbricata*,
524 since germination usually coincides with late-summer rains (*T.E.X. Miller, un-*
525 *publ. data*). Because we did not model this process as climate-dependent, our
526 results for climate effects on population growth are conservative. However, con-
527 sistent with expectations for long-lived perennials, we know seedling recruitment
528 to have very low eigenvalue sensitivities (Elder & Miller, 2016), which suggests
529 that even large climate effects on this process may not strongly register in terms

530 of population growth, as we observed for the reproductive functions of established
531 plants (Fig. 4B).

532 A second limitation is that our approach to quantifying climate drivers know-
533 ingly forfeits some information, and in two ways. First, in order to gain deep
534 temporal coverage, we relied on downscaled climate projections rather than di-
535 rect climatological observations. While we know these two types of data to be
536 highly correlated (Fig. A1), they are not perfectly so; this is especially true for
537 temperature minima and maxima (Table A1), where downscaled data likely mis-
538 estimate localized extremes. It is noteworthy that the downscaled climate data
539 poorly captured the extreme deep-freeze of winter 2011 (Fig. A1). Poor de-
540 mographic performance in this year was consequently attributed to a statistical
541 random effect (Fig. 4A), though this was almost certainly a true climate effect.
542 Second, we limited our consideration of climate drivers to the first three principal
543 components of inter-annual variation. While these three components explained a
544 large majority of the variation (Fig. 1A), we are disregarding some of the more
545 subtle dimensions of climate variability and change. Given our main finding that
546 the strongest features of climate change are not the main determinants of popu-
547 lation responses, these neglected dimensions may include important demographic
548 drivers. These two factors mean that our conclusions for climate-dependence err
549 on the conservative side.

550 To conclude, this study illustrates how long-term patterns of population vi-
551 ability can be reconstructed through climate-demography relationships observed
552 on relatively short time scales. This allowed us to evaluate the hypothesis that
553 recent climate change has driven *C. imbricata* in our region into extinction debt,
554 a hypothesis that we soundly reject. Instead, this species is most likely a cli-

555 mate change winner, largely due to its positive responses, especially in survival,
556 to recent and ongoing shifts in cool-season temperature and precipitation. Inter-
557 estingly, changes in cool-season climate were not the strongest features of climate
558 change, but they were nonetheless the most important determinants of population
559 responses. The more general lesson for global change biologists is that relatively
560 subtle dimensions of climate change may trigger strong ecological responses.

561 **Acknowledgements**

562 This study was supported by the Sevilleta LTER (NSF LTER awards 1440478,
563 1655499, and 1748133) and by NSF-DEB-1754468. We thank U.S Fish and Wildlife
564 Service staff (especially J. Erz) for facilitating research access to Sevilleta NWR.
565 We thank M. Evans and E. Schultz for helpful discussions on modeling climate-
566 demography relationships. Finally, we thank the many students and colleagues
567 have contributed to long-term data collection, especially M. Donald and B. Ochocki.

568 **Author contributions**

569 TEXM initiated and maintains the long-term study. KC collected and analyzed
570 data and prepared a manuscript draft. TEXM finalized text and analyses. Both
571 coauthors approve this submission.

Data accessibility

All of the code for our statistical and demographic modeling is available at https://github.com/texmiller/cholla_climate_IPM and raw data will be published in parallel with this manuscript.

References

- Ådahl E, Lundberg P, Jonzen N (2006) From climate change to population change: the need to consider annual life cycles. *Global Change Biology*, **12**, 1627–1633.
- Adams DK, Comrie AC (1997) The north american monsoon. *Bulletin of the American Meteorological Society*, **78**, 2197–2214.
- Adler PB, Byrne KM, Leiker J (2013) Can the past predict the future? experimental tests of historically based population models. *Global change biology*, **19**, 1793–1803.
- Allen L, Allen E, Kunst C, Sosebee R (1991) A diffusion model for dispersal of *Opuntia imbricata* (cholla) on rangeland. *The Journal of Ecology*, pp. 1123–1135.
- Bowers JE (2005) Influence of climatic variability on local population dynamics of a sonoran desert *Platyopuntia*. *Journal of Arid Environments*, **61**, 193–210.
- Boyce MS, Haridas CV, Lee CT, Group NSDW, *et al.* (2006) Demography in an increasingly variable world. *Trends in Ecology & Evolution*, **21**, 141–148.
- Buckley LB, Kingsolver JG (2012) The demographic impacts of shifts in climate means and extremes on alpine butterflies. *Functional Ecology*, **26**, 969–977.

- 592 Caswell H (2001) *Matrix Population Models*. Sinauer Associates, Inc., Sunderland,
593 MA, 2 edn.
- 594 Compagnoni A, Bibian AJ, Ochocki BM, *et al.* (2016) The effect of demographic
595 correlations on the stochastic population dynamics of perennial plants. *Ecolog-
596 ical Monographs*, **86**, 480–494.
- 597 Cook B, Seager R (2013) The response of the north american monsoon to increased
598 greenhouse gas forcing. *Journal of Geophysical Research: Atmospheres*, **118**,
599 1690–1699.
- 600 Cook BI, Ault TR, Smerdon JE (2015) Unprecedented 21st century drought risk
601 in the american southwest and central plains. *Science Advances*, **1**, e1400082.
- 602 Crone EE, Menges ES, Ellis MM, *et al.* (2011) How do plant ecologists use matrix
603 population models? *Ecology letters*, **14**, 1–8.
- 604 Dahlgren JP, Bengtsson K, Ehrlén J (2016) The demography of climate-driven and
605 density-regulated population dynamics in a perennial plant. *Ecology*.
- 606 Dalglish HJ, Koons DN, Adler PB (2010) Can life-history traits predict the re-
607 sponse of forb populations to changes in climate variability? *Journal of Ecology*,
608 **98**, 209–217.
- 609 Dalglish HJ, Koons DN, Hooten MB, Moffet CA, Adler PB (2011) Climate influ-
610 ences the demography of three dominant sagebrush steppe plants. *Ecology*, **92**,
611 75–85.
- 612 Daly C, Halbleib M, Smith JI, *et al.* (2008) Physiographically sensitive mapping
613 of climatological temperature and precipitation across the conterminous united

- 614 states. *International Journal of Climatology: a Journal of the Royal Meteorological Society*, **28**, 2031–2064.
- 615
- 616 Dinno A (2018) *paran: Horn's Test of Principal Components/Factors*. URL <https://CRAN.R-project.org/package=paran>. R package version 1.5.2.
- 617
- 618 Doak DF, Morris WF (2010) Demographic compensation and tipping points in
- 619 climate-induced range shifts. *Nature*, **467**, 959.
- 620 Dullinger S, Gatttringer A, Thuiller W, *et al.* (2012) Extinction debt of high-
- 621 mountain plants under twenty-first-century climate change. *Nature Climate*
- 622 *Change*, **2**, 619.
- 623 Dybala KE, Eadie JM, Gardali T, Seavy NE, Herzog MP (2013) Projecting de-
- 624 mographic responses to climate change: adult and juvenile survival respond
- 625 differently to direct and indirect effects of weather in a passerine population.
- 626 *Global Change Biology*, **19**, 2688–2697.
- 627 Ehrlén J, Morris WF (2015) Predicting changes in the distribution and abundance
- 628 of species under environmental change. *Ecology Letters*, **18**, 303–314.
- 629 Ehrlén J, Morris WF, von Euler T, Dahlgren JP (2016) Advancing environmentally
- 630 explicit structured population models of plants. *Journal of Ecology*, **104**, 292–
- 631 305.
- 632 Elderd BD, Miller TE (2016) Quantifying demographic uncertainty: Bayesian
- 633 methods for integral projection models. *Ecological Monographs*, **86**, 125–144.
- 634 Flores JL, Yeaton R (2003) The replacement of arborescent cactus species along a

635 climatic gradient in the southern chihuahuan desert: competitive hierarchies and
636 response to freezing temperatures. *Journal of arid environments*, **55**, 583–594.

637 Franco M, Silvertown J (2004) A comparative demography of plants based upon
638 elasticities of vital rates. *Ecology*, **85**, 531–538.

639 Franklin SB, Gibson DJ, Robertson PA, Pohlmann JT, Fralish JS (1995) Parallel
640 analysis: a method for determining significant principal components. *Journal of*
641 *Vegetation Science*, **6**, 99–106.

642 Frederiksen M, Daunt F, Harris MP, Wanless S (2008) The demographic impact
643 of extreme events: stochastic weather drives survival and population dynamics
644 in a long-lived seabird. *Journal of Animal Ecology*, **77**, 1020–1029.

645 George EI, McCulloch RE (1993) Variable selection via gibbs sampling. *Journal*
646 *of the American Statistical Association*, **88**, 881–889.

647 González-Varo JP, Albaladejo RG, Aizen MA, Arroyo J, Aparicio A (2015) Ex-
648 tinction debt of a common shrub in a fragmented landscape. *Journal of Applied*
649 *Ecology*, **52**, 580–589.

650 Hastings A, Abbott KC, Cuddington K, *et al.* (2018) Transient phenomena in
651 ecology. *Science*, **361**, eaat6412.

652 Hijmans RJ, Cameron SE, Parra JL, Jones PG, Jarvis A (2005) Very high reso-
653 lution interpolated climate surfaces for global land areas. *International Journal*
654 *of Climatology: A Journal of the Royal Meteorological Society*, **25**, 1965–1978.

655 Hooten MB, Hobbs N (2015) A guide to bayesian model selection for ecologists.
656 *Ecological Monographs*, **85**, 3–28.

- 657 Hylander K, Ehrlén J (2013) The mechanisms causing extinction debts. *Trends in*
658 *ecology & evolution*, **28**, 341–346.
- 659 Iler AM, Compagnoni A, Inouye DW, Williams JL, CaraDonna PJ, Anderson
660 A, Miller TE (2019) Reproductive losses due to climate change-induced earlier
661 flowering are not the primary threat to plant population viability in a perennial
662 herb. *Journal of Ecology*, **107**, 1931–1943.
- 663 Jenouvrier S, Caswell H, Barbraud C, Holland M, Stroeve J, Weimerskirch H (2009)
664 Demographic models and ipcc climate projections predict the decline of an em-
665 peror penguin population. *Proceedings of the National Academy of Sciences*,
666 **106**, 1844–1847.
- 667 Jenouvrier S, Holland M, Stroeve J, Serreze M, Barbraud C, Weimerskirch H,
668 Caswell H (2014) Projected continent-wide declines of the emperor penguin un-
669 der climate change. *Nature Climate Change*, **4**, 715.
- 670 Kinraide TB (1978) The ecological distribution of cholla cactus (*opuntia imbricata*
671 (haw.) dc.) in el paso county, colorado. *The Southwestern Naturalist*, pp. 117–
672 133.
- 673 Kuussaari M, Bommarco R, Heikkinen RK, *et al.* (2009) Extinction debt: a chal-
674 lenge for biodiversity conservation. *Trends in ecology & evolution*, **24**, 564–571.
- 675 Lehtilä K, Dahlgren JP, Garcia MB, Leimu R, Syrjänen K, Ehrlén J (2016) For-
676 est succession and population viability of grassland plants: long repayment of
677 extinction debt in *primula veris*. *Oecologia*, **181**, 125–135.
- 678 Lynch HJ, Rhainds M, Calabrese JM, Cantrell S, Cosner C, Fagan WF (2014) How

679 climate extremes—not means—define a species’ geographic range boundary via
 680 a demographic tipping point. *Ecological Monographs*, **84**, 131–149.

681 Maschinski J, Baggs JE, QUINTANA-ASCENCIO PF, Menges ES (2006) Using
 682 population viability analysis to predict the effects of climate change on the ex-
 683 tinction risk of an endangered limestone endemic shrub, arizona cliffrose. *Con-*
 684 *servation Biology*, **20**, 218–228.

685 McLean N, Lawson CR, Leech DI, van de Pol M (2016) Predicting when climate-
 686 driven phenotypic change affects population dynamics. *Ecology Letters*, **19**,
 687 595–608.

688 Miller TE, Louda SM, Rose KA, Eckberg JO (2009) Impacts of insect herbivory on
 689 cactus population dynamics: experimental demography across an environmental
 690 gradient. *Ecological Monographs*, **79**, 155–172.

691 Morris WF, Pfister CA, Tuljapurkar S, *et al.* (2008) Longevity can buffer plant and
 692 animal populations against changing climatic variability. *Ecology*, **89**, 19–25.

693 Morrison SF, Hik DS (2007) Demographic analysis of a declining pika ochotona
 694 collaris population: linking survival to broad-scale climate patterns via spring
 695 snowmelt patterns. *Journal of Animal ecology*, **76**, 899–907.

696 Nobel PS (1984) Extreme temperatures and thermal tolerances for seedlings of
 697 desert succulents. *Oecologia*, **62**, 310–317.

698 Notaro M, Gutzler D (2012) Simulated impact of vegetation on climate across the
 699 north american monsoon region in ccs3. 5. *Climate dynamics*, **38**, 795–814.

- 700 Ogle K, Barber JJ, Barron-Gafford GA, *et al.* (2015) Quantifying ecological mem-
701 ory in plant and ecosystem processes. *Ecology letters*, **18**, 221–235.
- 702 Ohm JR, Miller TE (2014) Balancing anti-herbivore benefits and anti-pollinator
703 costs of defensive mutualists. *Ecology*, **95**, 2924–2935.
- 704 Peters DP, Havstad KM, Archer SR, Sala OE (2015) Beyond desertification: new
705 paradigms for dryland landscapes. *Frontiers in Ecology and the Environment*,
706 **13**, 4–12.
- 707 Petrie M, Collins S, Gutzler D, Moore D (2014) Regional trends and local variabil-
708 ity in monsoon precipitation in the northern chihuahuan desert, usa. *Journal of*
709 *arid environments*, **103**, 63–70.
- 710 Pfister CA (1998) Patterns of variance in stage-structured populations: evolution-
711 ary predictions and ecological implications. *Proceedings of the National Academy*
712 *of Sciences*, **95**, 213–218.
- 713 Plummer M, *et al.* (2003) Jags: A program for analysis of bayesian graphical
714 models using gibbs sampling. In: *Proceedings of the 3rd international workshop*
715 *on distributed statistical computing*, vol. 124. Vienna, Austria.
- 716 Rudgers JA, Chung YA, Maurer GE, Moore DI, Muldavin EH, Litvak ME, Collins
717 SL (2018) Climate sensitivity functions and net primary production: A frame-
718 work for incorporating climate mean and variability. *Ecology*, **99**, 576–582.
- 719 Salguero-Gomez R, Siewert W, Casper BB, Tielbörger K (2012) A demographic
720 approach to study effects of climate change in desert plants. *Philosophical Trans-*
721 *actions of the Royal Society B: Biological Sciences*, **367**, 3100–3114.

- 722 Selwood KE, McGeoch MA, Mac Nally R (2015) The effects of climate change
723 and land-use change on demographic rates and population viability. *Biological*
724 *Reviews*, **90**, 837–853.
- 725 Shriver RK (2016) Quantifying how short-term environmental variation leads to
726 long-term demographic responses to climate change. *Journal of Ecology*, **104**,
727 65–78.
- 728 Sletvold N, Dahlgren JP, Øien DI, Moen A, Ehrlén J (2013) Climate warming alters
729 effects of management on population viability of threatened species: results from
730 a 30-year experimental study on a rare orchid. *Global Change Biology*, **19**, 2729–
731 2738.
- 732 Smith M, Caswell H, Mettler-Cherry P (2005) Stochastic flood and precipitation
733 regimes and the population dynamics of a threatened floodplain plant. *Ecological*
734 *Applications*, **15**, 1036–1052.
- 735 Su YS, Yajima M (2012) R2jags: A package for running jags from r. *R package*
736 *version 0.03-08*, URL <http://CRAN.R-project.org/package=R2jags>.
- 737 Teller BJ, Adler PB, Edwards CB, Hooker G, Ellner SP (2016) Linking demogra-
738 phy with drivers: climate and competition. *Methods in Ecology and Evolution*,
739 **7**, 171–183.
- 740 Tenhumberg B, Crone EE, Ramula S, Tyre AJ (2018) Time-lagged effects of
741 weather on plant demography: drought and astragalus scaphoides. *Ecology*,
742 **99**, 915–925.

- Urban MC (2015) Accelerating extinction risk from climate change. *Science*, **348**, 571–573.
- Van de Pol M, Vindenes Y, Sæther BE, Engen S, Ens BJ, Oosterbeek K, Tinbergen JM (2010) Effects of climate change and variability on population dynamics in a long-lived shorebird. *Ecology*, **91**, 1192–1204.
- Vellend M, Verheyen K, Jacquemyn H, Kolb A, Van Calster H, Peterken G, Hermy M (2006) Extinction debt of forest plants persists for more than a century following habitat fragmentation. *Ecology*, **87**, 542–548.
- Villellas J, Doak DF, García MB, Morris WF (2015) Demographic compensation among populations: what is it, how does it arise and what are its implications? *Ecology letters*, **18**, 1139–1152.
- Wang T, Hamann A, Spittlehouse D, Carroll C (2016) Locally downscaled and spatially customizable climate data for historical and future periods for north america. *PLoS One*, **11**, e0156720.
- Williams JL, Jacquemyn H, Ochocki BM, Brys R, Miller TE (2015) Life history evolution under climate change and its influence on the population dynamics of a long-lived plant. *Journal of Ecology*, **103**, 798–808.
- Williams JL, Miller TEX, Ellner SP (2012) Avoiding unintentional eviction from integral projection models. *Ecology*, **93**, 2008–2014.
- Winkler DE, Conner JL, Huxman TE, Swann DE (2018) The interaction of drought and habitat explain space–time patterns of establishment in saguaro (*Carnegiea gigantea*). *Ecology*, **99**, 621–631.

765 Yu K, D’Odorico P, Collins SL, *et al.* (2019) The competitive advantage of a con-
766 stitutive cam species over a c4 grass species under drought and co2 enrichment.
767 *Ecosphere*, **10**, e02721.

768 Appendix A: Correspondence between downscaled 769 and locally measured climate variables

770 We compared warm- and cool-season values of four climate variables (total pre-
771 cipitation and minimum, mean, and maximum temperature) between two data
772 sources: the SEV-LTER meteorological station nearest our study site (station 50 in
773 the SEV-LTER meteorological network) and downscaled data from ClimateWNA
774 corresponding to the same latitude, longitude, and elevation as station 50. Our
775 goal was to determine how well the downscaled data captured conditions ‘on the
776 ground’ as measured directly by the meteorological station. We compared the
777 years 2001 through 2017, which are the years of overlap between the two data
778 sources.

779 There was generally strong agreement between the two data sources (Table A1,
780 Figure A1). Temperature extrema were less strongly correlated between the two
781 data sets than temperature means, which is unsurprising given that extreme values
782 may be sensitive to local micro-environmental conditions that the relatively coarse
783 downscaled data would miss. The weakest correlation was that of warm-season
784 maximum temperature (Spearman’s $r = 0.41$, $P = 0.11$).

Table A1: Correlations between seasonal climate values measured by an on-site meteorological station versus downscaled data from ClimateWNA corresponding to the same years and location. Correlation values show Pearson correlations and P-values come from t -tests with 14 degrees of freedom.

Season	Variable	Correlation	P-value
Warm	Min temperature	0.59	0.0153
Warm	Mean temperature	0.84	10^{-4}
Warm	Max temperature	0.41	0.1135
Warm	Precipitation	0.49	0.0544
Cool	Min temperature	0.51	0.0622
Cool	Mean temperature	0.94	3.6×10^{-7}
Cool	Max temperature	0.69	0.0069
Cool	Precipitation	0.87	4.6×10^{-5}

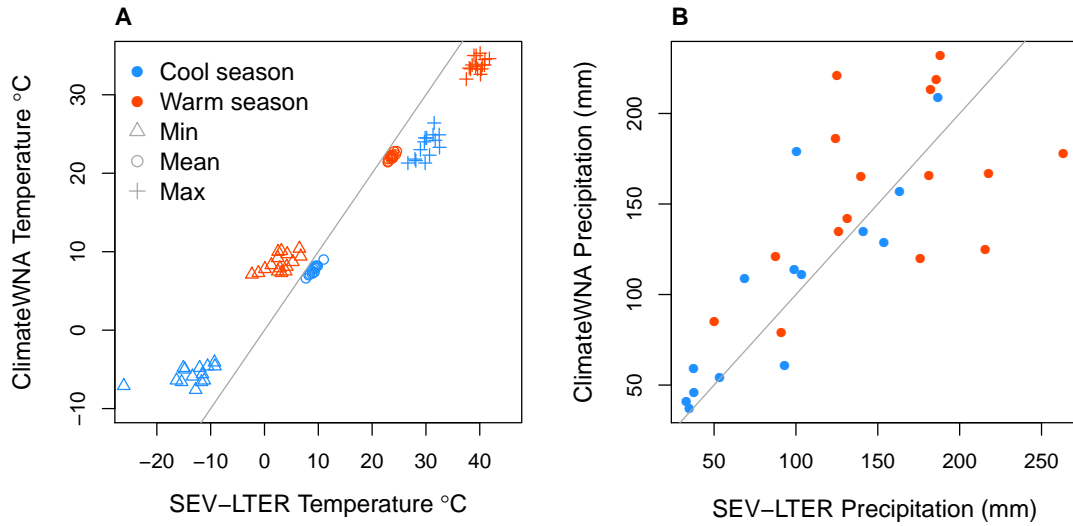


Figure A1: Correlations between seasonal climate values (**A**: temperature; **B**: precipitation) between SEV-LTER meteorological data and downscaled estimates from ClimateWNA for years 2001–2017. Gray lines show $y = x$.

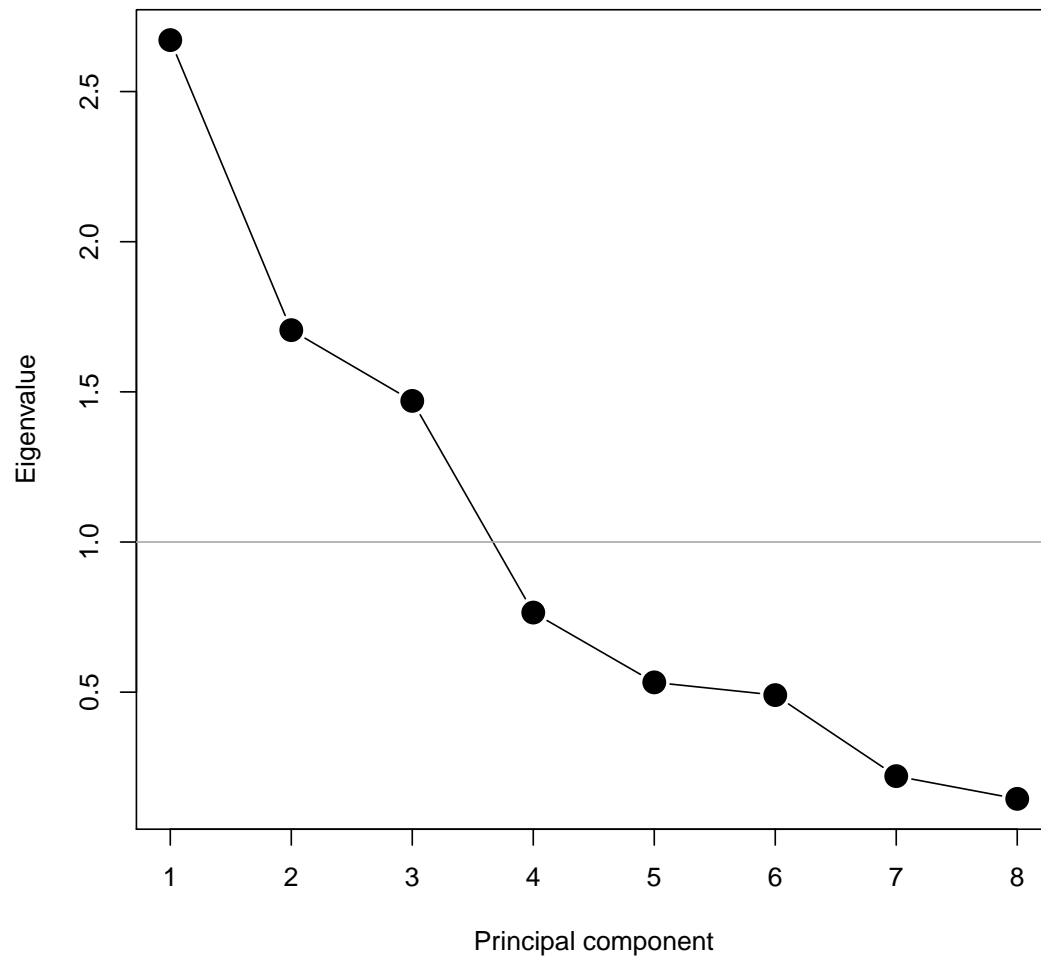


Figure A2: Results of parallel analysis conducted using the R package ‘paran’ (Dinno, 2018). Components with eigenvalues greater than 1 are retained.

Appendix B: Stochastic variable selection

Because we intended to extrapolate the vital rate models into past climate environments that were not well represented during the long-term study, it was important that we simplify the vital rate models to exclude unnecessary coefficients (which, even if small in absolute value, could generate unrealistic predictions when extrapolated over a greater range of climate than the models were fitted to). To do this, we used stochastic variable selection, a ‘model-based model selection’ approach (Hooten & Hobbs, 2015) that generates weightings for each fixed-effect coefficient, indicating the probability that the coefficient is non-zero. We employed an approach based on George and McCulloch (1993) where each coefficient (C_i) is modeled as a mixture distribution with zero and non-zero modes, where modal frequency is determined by an indicator variable (z_i). The coefficient prior was:

$$C_i \sim (1 - z_i) * N(0, 0.1) + z_i * N(0, 1000) \quad (\text{B1})$$

$$z_i \sim \text{Bernoulli}(0.5) \quad (\text{B2})$$

The first term of the mixture distribution assigns, with probability $(1 - z_i)$, a prior with mean zero and arbitrarily small variance, effectively forcing the posterior estimate to equal zero. The second term assigns, with probability z_i , a prior with mean zero and arbitrarily large variance, which allows for a non-zero posterior estimate. The posterior distribution of the indicator variable z_i gives the probability that the coefficient is non-zero. We estimated this probability for each coefficient in Eq. B1 and retained in the final model all coefficients with a posterior

mean $\hat{z}_i > 0.1$, meaning that the model term is determined to be non-zero with
90% confidence. All z_i values from the full model are shown in Table B1.

Climate PC	Model term	Survival	Growth	Flowering	Fertility
	Size	1	0.53	1	1
1	PC	0.13	0.04	0.12	0.05
1	PC*PC	0.03	0.01	0.03	0.01
1	PC*size	0.06	0.01	0.08	0.07
2	PC	0.18	0.03	0.11	0.14
2	PC*PC	0.06	0.01	0.06	0.03
2	PC*size	0.04	0.02	1	0.27
3	PC	0.18	0.02	0.12	0.18
3	PC*PC	0.09	0.01	0.09	0.06
3	PC*size	0.06	0.01	0.13	0.03

Table B1: Stochastic variable selection results. Values (z) can be interpreted as the probability that a model coefficient is non-zero. Bolded values indicate terms retained in the final model.

806 Appendix C: Additional demographic modeling meth- 807 ods and results

808 We estimated a time series for the stochastic population growth rate (λ_S) over
809 the period 1900-2017 using a moving window approach. While the determinis-
810 tic growth rate for each year estimates the long-run growth rate expected if the
811 conditions of that year remained constant, the stochastic growth rate integrated
812 over a broader range of conditions, incorporating year-to-year fluctuations and
813 auto-correlation of climate variables.

We simulated population dynamics according to Equations 4–2 to estimate the stochastic population growth rate λ_S . We estimated λ_S for 10-year windows spanning the time series 1901–2017, such that the value of λ_S for year t reflects the stochastic growth rate for a climate environment defined by years t through $t + 9$. For each 10-year window, we simulated 1000 years of population dynamics, each year randomly drawing one of the 10 climate-years. For each year of the simulation, we calculated total population size as:

$$N_t = \int n(x)_t dx + B_{1,t} + B_{2,t} \quad (\text{C1})$$

and estimated the stochastic growth rate for that window as the expected value of the one-year growth rate:

$$\log(\lambda_S) = \mathbb{E}[\log(\frac{N_{t+1}}{N_t})] \quad (\text{C2})$$

Table C1: Parameter values of tree cholla IPM.

Parameter description	Symbol	Mean	95%CI
Survival coefficients	β_0	3.33	(1.4 – 5.25)
	β_1	1.31	(1.18 – 1.44)
	ρ_1^1	-0.11	(-0.82 – 0.61)
	ρ_1^2	0.41	(-0.25 – 1.13)
	ρ_1^3	-0.28	(-0.84 – 0.3)
Growth coefficients	β_0	-0.03	(-0.08 – 0.02)
	β_1	-0.02	(-0.03 – -0.02)
Growth standard deviation	σ	0.25	(0.25 – 0.26)
Flowering coefficients	β_0	-4.76	(-7.37 – -2.22)
	β_1	5.17	(4.78 – 5.54)
	ρ_1^1	-0.26	(-1.27 – 0.7)
	ρ_1^2	0.07	(-0.85 – 1.01)
	ρ_3^2	1.11	(0.65 – 1.61)
	ρ_1^3	-0.04	(-0.79 – 0.77)
	ρ_3^3	0.21	(-0.06 – 0.47)
Fertility coefficients	β_0	-0.25	(-0.6 – 0.1)
	β_1	2.22	(2.01 – 2.42)
	ρ_1^2	0.06	(-0.15 – 0.28)
	ρ_3^2	0.17	(-0.01 – 0.35)
	ρ_1^3	0.12	(-0.04 – 0.29)
Seeds per fruit	κ	113.46	(93.47 – 132.59)
Recruitment into seed bank	δ	0.03	(0.02 – 0.05)
Germination rates	γ_1	0.0059	(0.0047 – 0.0073)
	γ_2	0.0044	(0.0033 – 0.0056)
Seedling size distribution	μ_s	-3.49	(-3.62 – -3.37)
	σ_s	0.23	(0.15 – 0.35)
Seedling survival	ω	0.5	(0.002 – 0.998)
Size bounds	L	-3.94	
	U	1.89	

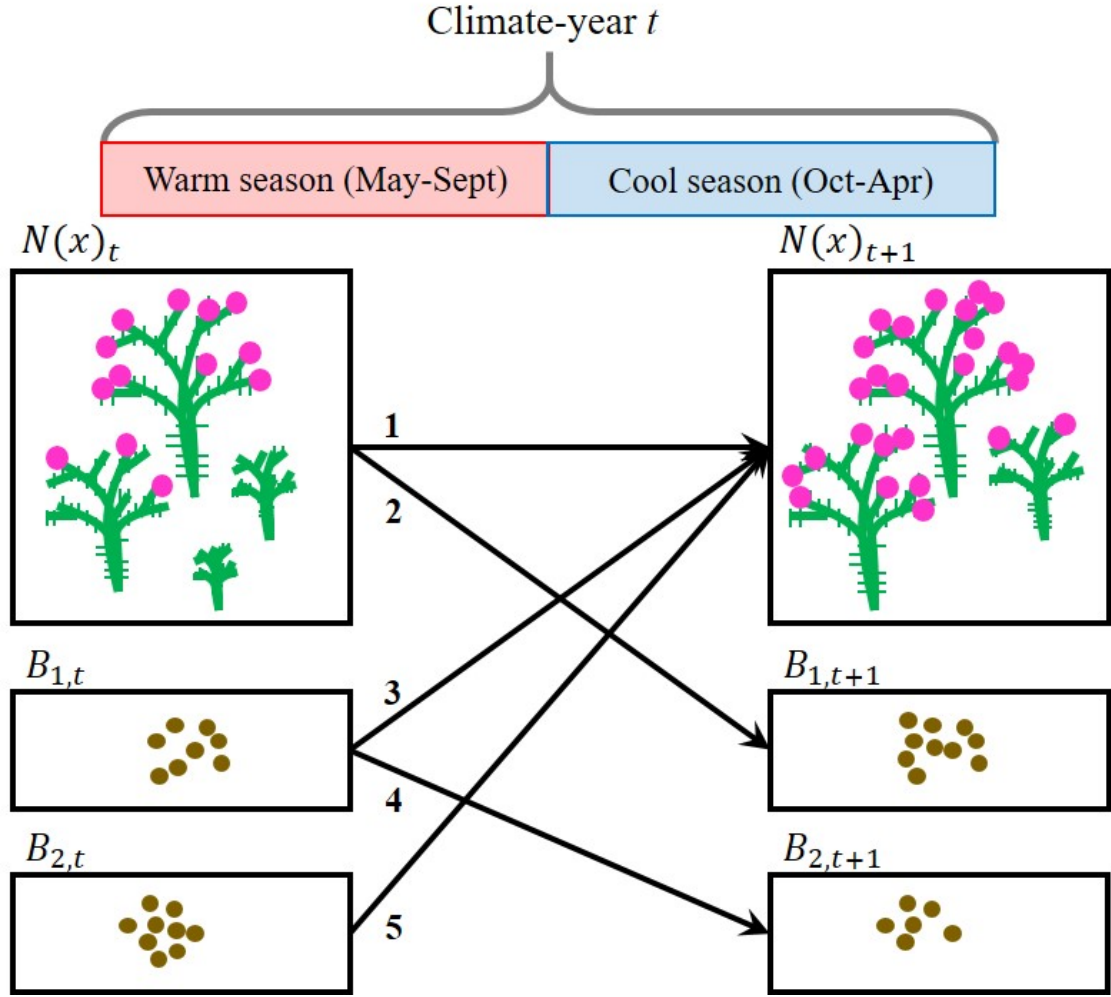


Figure C1: *C. imbricata* life cycle and census timing with respect to warm- and cool-season climate. Numbered arrows correspond to demographic events that occur during a transition year: (1) established plants survive and grow, (2) plants that are reproductive in year t contribute seeds that will make up the 1-yo seed bank in year $t+1$, (3) a fraction of seeds in the 1-yo seed bank survive and recruit into the plant population as seedlings in year $t+1$, (4) another fraction of seeds in the 1-yo seed bank survives and remains to form the 2-yo seed bank in year $t+1$, (5) a fraction of seeds in the 2-yo seed bank survive and recruit into the plant population as seedlings in year $t+1$. Survival and growth from year t to year $t+1$ (arrow 1) depended on climate year year t , whereas flowering and flowerbud production in year t (components of arrow 2) depended on climate in year $t-1$.

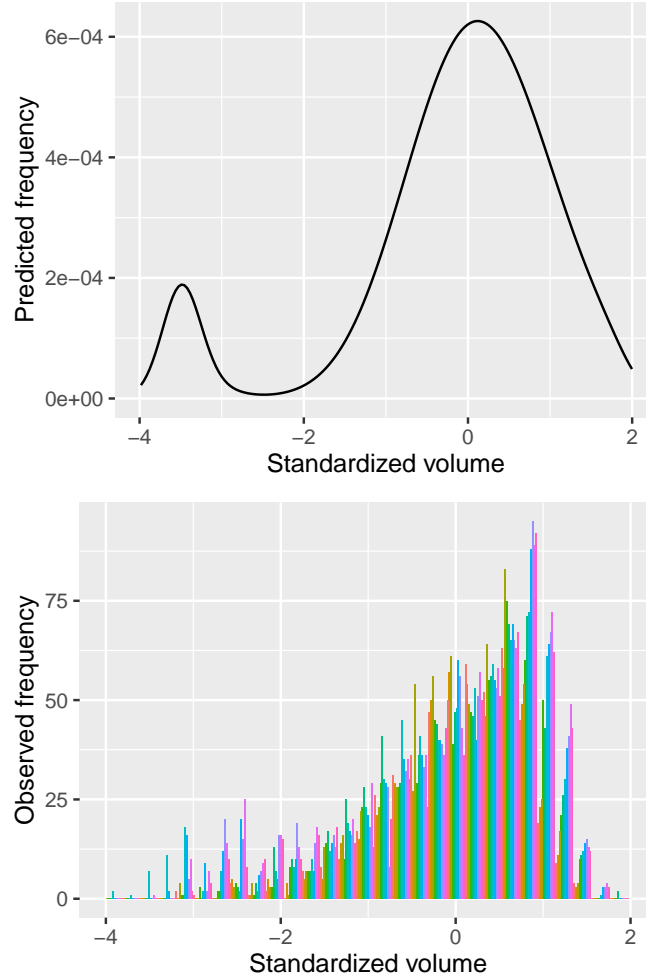


Figure C2: Comparison of predicted (top) and observed (bottom) size distributions, where size was the natural logarithm of plant volume standardized to mean zero. In the bottom panel, different colors represent different years. The predicted stable size distribution (evaluated at the average climate) corresponded well to the observed size distribution, though very large plants were over-represented in the observed distribution. This is consistent with the idea that the population may have recently transitioned into decline, whereby the persistence of large plants may reflect a legacy of positive growth rates. Also, the peak for new recruits was at a larger size in the observed distribution, but this was likely a consequence of the fact that we rarely detected new recruits. The “new” plants in our plots each year were likely several years old.

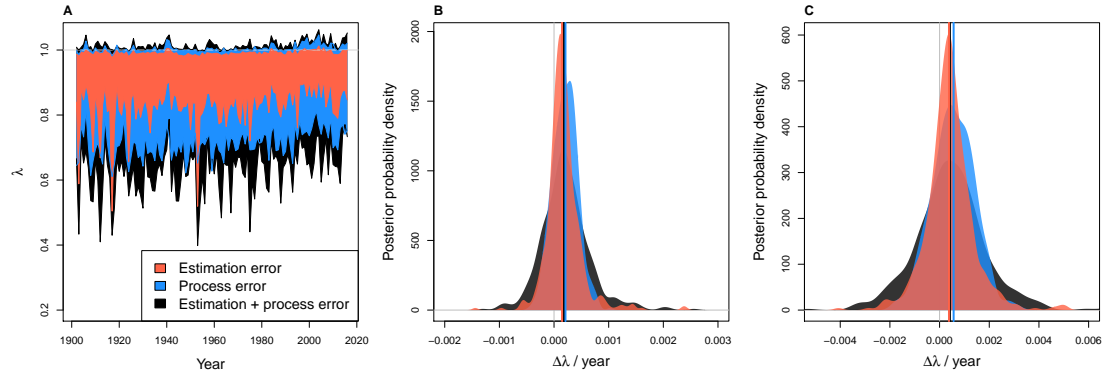


Figure C3: **A**, Time series of back-casted asymptotic population growth rates (λ) predicted based on inter-annual variation in three climate PCs. Shaded regions show the 95% credible interval of the posterior probability distributions for three uncertainty scenarios: estimation error only (parameter uncertainty; red), process error only (year-to-year heterogeneity unrelated to the climate PCs; blue), and both estimation and process error (black). **B**, **C**, Posterior probability distribution for the change in λ per year based on the entire time series (**B**) or years since 1970 (**C**). Vertical lines show the medians of the posterior distributions. Colors as in **A**.

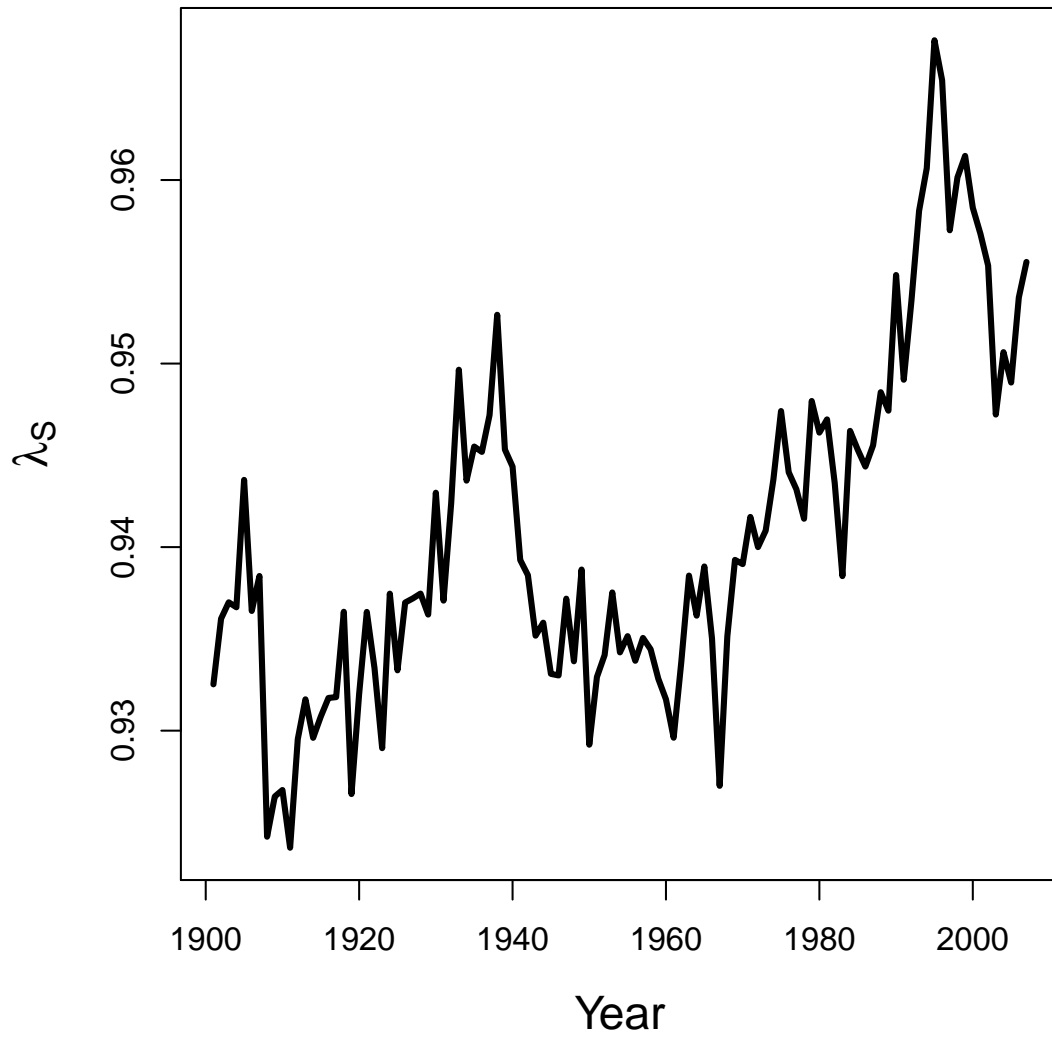


Figure C4: Time series of stochastic population growth rates (λ_S). Values are based on a 10-year sliding window such that λ_S is year t is based on the climate regime over the years t through $t + 9$

814 Appendix D: Exploring the consequences of climate 815 extrapolation

816 Our analysis in the main text relied on extrapolating demographic responses to
817 climate into climate environments that were not directly observed during our field
818 study. For example, high values of PC1 and low values of PC2 were under-
819 represented during the study years (Fig. D1). We explored the consequences
820 of this extrapolation by re-running our demographic analysis with bounds on cli-
821 mate responses. For each vital rate that responded to a climate PC according to
822 some function $f(PC)$, we defined a second function $f^*(PC)$ as:

$$f^*(PC) = \begin{cases} f(PC_L), & \text{if } PC < PC_L \\ f(PC_U), & \text{if } PC > PC_U \\ f(PC), & \text{otherwise} \end{cases} \quad (\text{D1})$$

823 where PC_L and PC_U are the lower and upper bounds, respectively, of the observed
824 range of PC values. For simulations into historical climates more extreme than
825 observed, this approach pins demographic responses to equal the responses at
826 observed extrema, as can be seen in λ responses to PC variation. We repeated our
827 back-casting analysis using this approach.

828 Results show that our qualitative results are not affected by climate extrapola-
829 tion. The back-casted time series of λ was generally consistent with and without
830 extrapolation (Fig. D3). The main differences were in the extreme low λ values,
831 which were lower with extrapolation. Both time series yielded a positive temporal
832 trend, though the mean change in λ per year was 35% weaker for the entire time

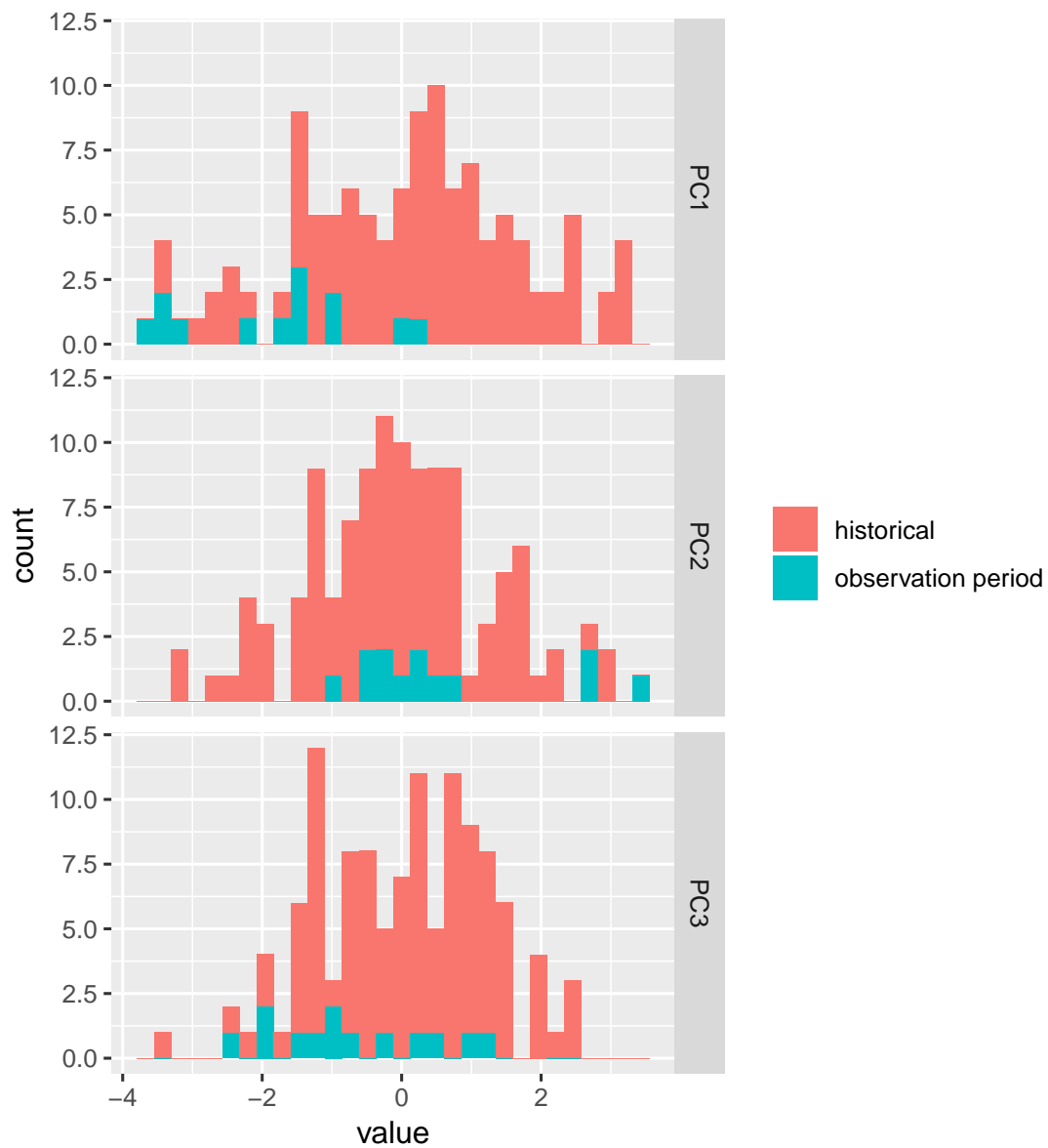


Figure D1: Distributions of observed climate values during the observation period (2004–2017) relative to historical values (1901–2016). Climate values are three principal components of inter-annual variation in cool- and warm-season temperature and precipitation.

833 series and 26% weaker since 1970 when vital rates were not extrapolated (Fig.
 834 D2). The limited influence of extrapolation was due to the fact that we relied

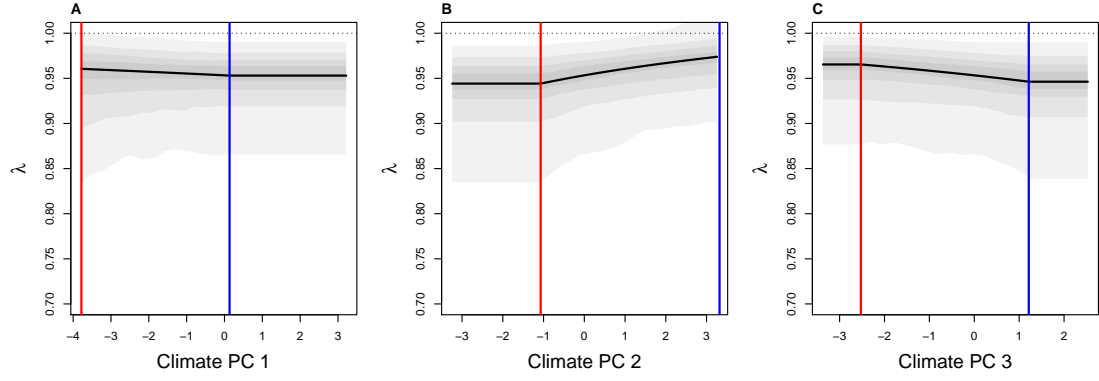


Figure D2: Relationships between λ and three climate PCs with no extrapolation into unobserved climate conditions. For PC values lower than the minimum (red vertical lines) and greater than the maximum (blue vertical lines) of the observation period, demographic responses were forced to match the extrema of the observation period according to Eq. D1.

835 most heavily on extrapolation for PC1 (Fig. D1). As we show in the main paper,
 836 this PC has changed the most during the historical record but it had the weakest
 837 effects on cactus demography.

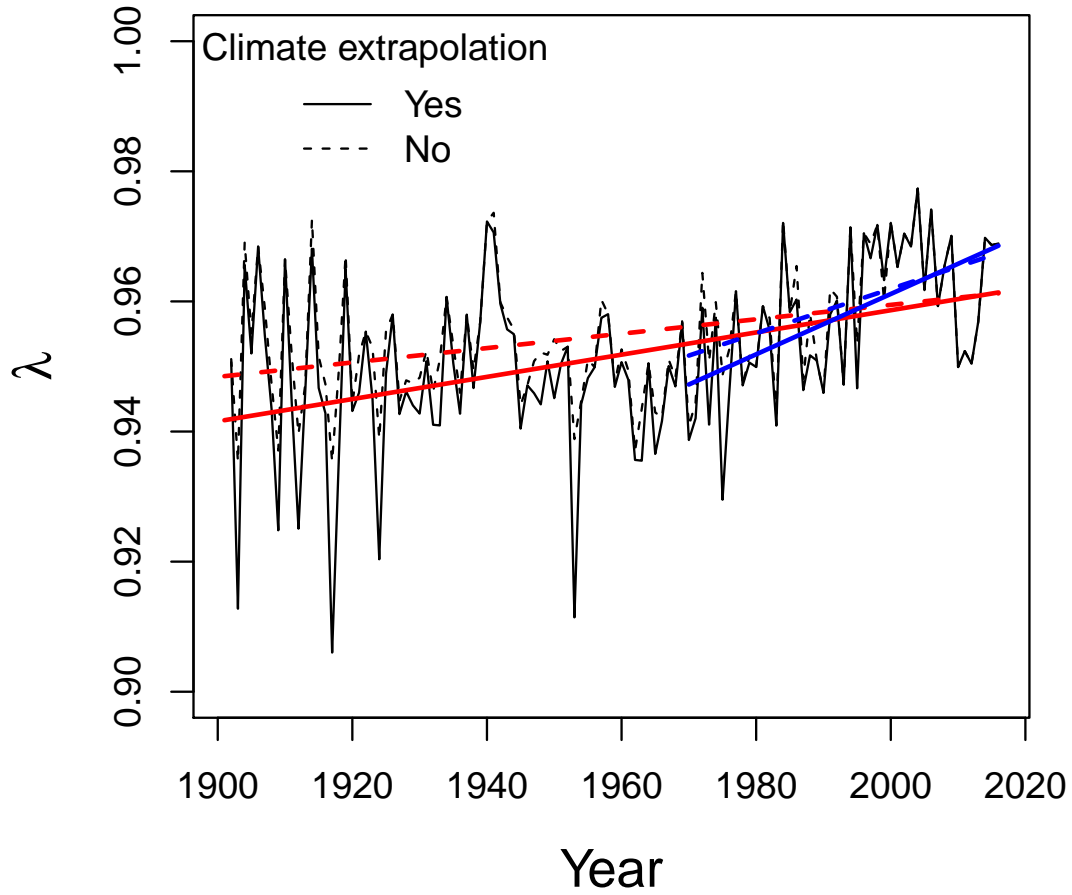


Figure D3: Back-casted values of climate-dependent population growth (λ) with (solid lines) and without (dashed lines) extrapolation of vital rate responses to unobserved climate conditions based on posterior mean parameter values. Red and blue lines show fitted regressions for the entire time series and since 1970, respectively.